THE UNIVERSITY OF MICHIGAN

COLLEGE OF ENGINEERING
Department of Meteorology and Oceanography

Technical Report

SATELLITE OBSERVATIONS RELATED TO ATMOSPHERIC PLANETARY WAVE DYNAMICS

James H. S. Bradley

Aksel C. Wiin-Nielsen
Project Director

ORA Project 08203

Supported by:

U. S. DEPARTMENT OF COMMERCE
ENVIRONMENTAL SCIENCE SERVICE ADMINISTRATION
WEATHER BUREAU
CONTRACT Cwb-11377
WASHINGTON, D.C.

administered through:

OFFICE OF RESEARCH ADMINISTRATION ANN ARBOR

February 1968

TABLE OF CONTENTS

TABLE OF CONTENTS (concluded)

ACKNOWLEDGMENTS

The author thanks the National Environmental Satellite Center, ESSA, for an office, computer, programmer, data and contract support from July to December 1967. Mr. A. Bedient of the National Meteorological Center provided stream functions. Mr. J. Winston discussed many of the results. Dr. Aksel Wiin-Nielsen directed work on the geopotential of the northern hemisphere, for which computing facilities were provided by The University of Michigan Computing Center. Dr. A. Robert asked many questions which the author hopes one day to answer.

The programming was done by Messrs. M. Chalfant, A. Pajas and H. Akfirat. Anything comprehensible in this report owes much to the professional editing of the author's wife, Estella. Miss Joan Shugarts typed the drafts and text.

LIST OF TABLES

LIST OF FIGURES

ABSTRACT

Previous observational results on the three dimensional structure of the free atmospheric planetary waves are similar to the gyroscopic (Rossby-Haurwitz) and gyroscopic-gravitational modes derived from the Laplace tidal equation by Dikii. Quantitative comparisons of the observed mode structure with the theories of Dikii, Matsuno, Lindzen, Marchuk and others awaits the publication of theoretical numerical values. It is suggested that the mode structure of the forced waves differs from that of the free waves because of the effects of terrain, friction, and diabatic effects. Vertical characteristic patterns of the stream function show the second vertical (H_2) mode to be relatively weak, and to have a marked meridional variation, and the H_1 mode to resemble the H_1 mode of the geopotential.

Satellite observations of cloud cover and brightness are used to show that the northern and southern hemispheres and the tropics are coupled, at least strongly enough to cause substantial correlations between systems close together in free period. Large exchanges of matter, momentum and energy are not necessarily implied. Modes confined to the tropics, and uncoupled middle latitude modes, account for 10 to 20% of the variance in their respective areas. At least one physical mechanism remains undiagnosed, which may be the vertical structure (H_2, L_1 mode).

An unpredicted conclusion is that the large scale cloudiness moves with approximately the Rossby-Haurwitz velocity of the first vertical (H_1) mode of the second meridional (L_2) mode of the geopotential; further work is needed to try to extract information about the most important meridional (L_1) and the second vertical (H_2) modes

of the geopotential from satellite cloud observations. Power spectra and vector correlations verify the suitability of an 11 day running mean time filter.

Zonal harmonics show definite advantages over other representations of the east-west structure.

Methodological improvements are presented in the representation of three dimensional characteristic patterns, in the estimation of uncoupled modes from variance explained, and in the numerical analysis of eigenvalues and eigenvectors of symmetric matrices. A notation for vertical and horizontal modes is introduced.

1. INTRODUCTION

1.1 OUTLINE

The observational study described in this report represents an attempt to apply current satellite cloud observations to the problems of the dynamics of the planetary waves in the tropics and southern hemisphere, and to quantify interactions between the middle latitudes of both hemispheres and the tropics.

The preliminary ideas of this study were derived from the author's Ph.D. thesis (Bradley and Wiin-Nielsen, 1967), which separated the planetary waves of the geopotential of the northern hemisphere into subclasses. The free transient quasi-nondivergent and free transient divergent subclasses appear to be approximately the gyroscopic (Rossby-Haurwitz) and gyroscopic-gravitational modes predicted by Dikii (1961, 1965), and both the standing and forced transient subclasses are attributable to the interactions of the free transient modes (Mashkovich, 1964; Holopainen, 1966), to diabatic effects (Blinova, 1943; Smagorinsky, 1953), to interactions of the flow with mountains (Charney and Eliasen, 1949), and to friction. The prediction of trapped tropical modes by Matsuno (1966) and Lindzen (1967) also suggested part of the work reported here.

Because the available linearized perturbation theories are known to contain grave approximations, and because the observational data yield more clear facts not predicted by published theories than crucial confrontations of different theories, dynamic theories and past observations are used mainly to suggest profitable tools and lines of enquiry. The methods used are statistical filtering techniques; the main justification for the conclusions is their

internal consistency and their ability to describe the observations. The results are independent of, and do not necessarily cast any light on, the theories which provided their original inspiration. In particular, current satellite cloud data give no information about the vertical structure of the atmosphere, and no attempt was made to distinguish cloud types or levels, nor to prepare geopotential or streamline analyses.

It was necessary to refine the available tools of time filtering, characteristic patterns (empirical orthogonal functions, natural functions or principal modes), expansion in analytically or empirically defined orthogonal functions, vector correlation, power spectra, structure functions and correlation functions by developing methods of selecting areas for characteristic pattern analysis (Appendix A). The characteristic pattern algorithms of the Jacobi method were refined by a third-order correction. The power method with orthogonalization was replaced by the power method with steepest descent, perturbation, and deflation or exhaustion (Fadeev and Fadeeva, 1960, describe all three). The power method was also used in techniques which the author calls purification and reorthogonalization, and original methods for the conditioning and inversion of ill-conditioned matrices were developed for use in the perturbation method.

1.2 PREVIOUS WORK

Among the authors who have recently studied the planetary waves from geopotential or stream function data by means of zonal or spherical harmonics are Deland (1965), Eliasen and Machenauer (1965), and Deland and Lin (1967). These authors found that the observed planetary waves at one or two pressure levels did not obey the Rossby-Haurwitz formula.

Bradley and Wiin-Nielsen (1967), working at eight pressure levels, in characteristic patterns, and with time filters, found a subclass of the planetary waves which move with the Rossby-Haurwitz speed with a plausible meridional scale. Other subclasses, not then explained, were the very slowly moving forced modes and the higher vertical and meridional modes. The vertical characteristic patterns of any wave agreed with those found by Holmstrom (1963); meridional characteristic patterns were common to the free modes irrespective of zonal wavenumber and vertical mode number. In the zonal direction, nothing significantly different from zonal harmonics was found.

Burger (1958) and Murakami (1963) developed scale analyses to demonstrate the internal consistency of quasi-stationary planetary waves, while Deland (1965) showed that the assumption of phase velocities in the order of the Rossby-Haurwitz speed is also self-consistent.

For lack of a convincing theory, some authors turned to computational models, from which Mashkovich (1964) predicted the existence of the forced modes and many aspects of the development and motion of planetary waves. Baer (1964) and Eliasen and Machenauer (1965) computed large non-linear effects on the instantaneous phase speeds, without, however, attempting to discover whether the mean value of the non-linear effects is zero, as was tacitly assumed by Bradley and Wiin-Nielsen (1967). Yang (1967) computed the mean effects of non-linear interactions on the kinetic energy of the planetary waves, but not on the mean phase speeds. Yang's calculations emphasize the great differences in the energetics of the free and forced modes. Many authors constructed diagnostic and prognostic models in the surface harmonics, without any theoretical conclusions

about the mechanisms of the planetary waves, e.g., Blinova (1943, 1964, 1965), Baer (1964), Robert (1965) and numerous others. Longuet-Higgins and Gill (1967) gave an analytical prediction of forced modes and triplet resonances among the planetary waves.

Yaglom (1953), Dikii (1961, 1965), and Golitsin and Dikii (1966) attempted to refine linearized perturbation theory on a sphere by taking account of the higher order terms in the Rossby number, and by including the vertical stratification of the atmosphere. These efforts have led to modifications of the order of 30% in the predictions of the Rossby-Haurwitz theory for the planetary waves, and more importantly have pointed to the class of gyroscopic-internal-gravity waves, which appear to have much in common with the observed, strongly divergent second vertical mode of Obukhov (1960), Holmström (1963) and Bradley and Wiin-Nielsen (1967). Details are given in Chapter 3. Charney (1947) took account of the vertical shear of the horizontal wind but found no new modes.

Derome and Wiin-Nielsen (1966) reviewed some theories of baroclinic instability, but these theories and the theories in spherical geometry (Mashkovich, 1961, 1964) introduce departures from the Rossby-Haruwitz speed no larger than the changes caused by the inclusion of higher order terms from the Laplace tidal equation.

Lindzen (1967) and Matsuno (1966) developed beta-plane approximations for the tropics with the basic Coriolis parameter zero, and predicted modes confined to the vicinity of the equator. Matsuno found modes which were a modification between Rossby and inertial-gravitational regimes.

Most recently, Marchuk (1965, 1967) has given a theory of linearization about a basic state in which the modes appear as the biorthogonal eigenfunctions of a non-self-adjoint linear operator.

1.3 AIM

The long range aims of this research, which are partly realized in this report, are:

1. To develop an automatic method of using satellite data in meteorological analyses and forecasts.
2. To this end, and for their own sakes, to understand the dynamics of the free (Rossby-Haurwitz and gyroscopic-gravitational), forced transient and stationary modes of the planetary waves.
3. To quantify and understand the meridional interactions, especially between the middle latitudes of both hemispheres and the tropics.
4. To detect and describe trapped tropical modes if they exist.
5. To determine the relations between the strongly divergent second vertical mode, cloudiness, and energy transformations.
6. To determine the thermodynamic roles and the maintenance of the observed characteristic patterns.

The possibilities of applying the classical scientific method of a crucial comparison between conflicting theories are restricted by the small number of resolvable conflicts between available theories of the planetary waves, and by our lack of control over the atmosphere. One may therefore attempt to verify or quantify the predictions of some theories, or one may hope that statistical filtering techniques will give such unequivocal results that there

can be no question of a well-defined phenomenon even if its mechanism is unknown; such a result was obtained by Obukhov (1960) and Holmström (1963) in the vertical, and extended by Bradley and Wiin-Nielsen (1967) in the horizontal. Further, numerical results have not been published for the theoretical vertical and meridional modes predicted by Dikii (1961, 1965), Golitsin and Dikii (1966), and Marchuk (1965, 1967); limited results are available for Matsuno (1966) and Lindzen (1967).

The following limited aims were chosen for this study:

1. To use available results on the geopotential to choose a time filter for the separation of free and forced planetary waves, and to check this choice by power spectrum analysis.
2. To determine the apparent phase velocities of time-filtered zonal and surface harmonics of the brightness and cloud cover, and subsequently to compare these with phase velocities obtained from the geopotential and stream function for the same time period. Only the apparent phase velocities are reported here.
3. To examine meridional characteristic patterns of the brightness and cloud cover for relations to the known patterns of the geopotential.
4. By examining characteristic patterns over selected latitude bands, to quantify interactions between the middle latitudes and the tropics.
5. To examine zonal correlations in order to quantify non-linear effects.
6. To examine zonal and meridional structure and correlation functions as support for other objectives and to aid in a comparison of characteristic pattern methods with conventional correlation techniques.

The objectives have been partly achieved by the development of new techniques and by the intensive application of well-established methods.

1.4 TOOLS

On the basis of available results for the long waves of the geopotential (Bradley and Wiin-Nielsen, 1967), an 11 day equally weighted running mean and the deviation from it were used throughout this study. The satisfactory separation of at least two classes of phenomena and power spectrum analysis justified this theory a posteriori. Programs were developed to compute the response of symmetric filters from prescribed weights or from a set of prescribed frequencies and responses. The theory of filters is described by Holloway (1958), but it is usually necessary to use trial and error, guided by a knowledge of the power spectrum or time auto-correlation function (Gandin, 1963).

The formalism of characteristic patterns (empirical orthogonal functions, natural functions, or principal modes is described by Bradley and Wiin-Nielsen (1967), Mateer (1965), Anderson (1958) and many others. The mean state is removed, and a covariance matrix generated; characteristic patterns describe only the fluctuations about a mean state. Once the square symmetric covariance matrix is obtained, identical results may be obtained by the methods of Jacobi or Givens, by steepest descent with deflation, or by the power method with re-orthogonalization, deflation and perturbation. The characteristic patterns are the eigenvectors X of the covariance matrix Y, and the variance explained by each pattern is proportional to the corresponding eigenvalue λ, where

$$YX = \lambda X. \qquad 1.4.1$$

Vector correlation is described by Ellison (1954), and discussed by Deland and Lin (1967). The author has not found any derivation of confidence limits for the estimates which vector correlation provides. Although vector regression may not handle discontinuities well, it is the only method for the machine estimation of mean angular velocities currently available.

Power spectra are discussed by Blackman and Tukey (1958): the method is sufficiently well known not to require description here.

Structure functions and correlation functions are described by Gandin (1963). The structure function of a parameter F is defined as

$$B_F(r_1, r_2) = \overline{[f(r_1) - f(r_2)]^2} \qquad 1.4.2$$

where r_1 and r_2 are position vectors, and the bar denotes averaging over a statistical ensemble (normally time).

The correlation function of two parameters F and Ø is defined as

$$M_{F\emptyset}(r_1, r_2) = \overline{f(r_1)\,\emptyset(r_2)} \qquad 1.4.3$$

Structure and correlation functions are most useful if their fields are statistically homogeneous and isotropic, i.e., a function only of the distance $|r_1 - r_2|$, but not of direction, nor of r_1 or r_2. Because the structure and correlation functions observed in this study are not even approximately homogeneous and isotropic, their uses are mainly qualitative.

2. DATA

2.1 GEOPOTENTIALS OF THE NORTHERN HEMISPHERE

The geopotential data used in this study are identical with those of Bradley and Wiin-Nielsen (1967), for the first six months of 1963. The treatment differs only in that the free transient modes are expanded in zonal harmonics and in the standard vertical and meridional characteristic patterns assigned by Bradley and Wiin-Nielsen (1967).

In this formulation a variable X is expressed as

$$X(\theta,\lambda,p,t) = \sum_{I}\sum_{J}\sum_{M} [A_N^M(t)\cos M\lambda + B_N^M(t) \sin M\lambda]H_I(p)\,L_j(\theta) \qquad 2.1.1$$

where A_N^M and B_N^M are coefficients; t is time; θ, co-latitude; λ, longitude; H is a pressure mode; and L, a latitudinal mode. H and L are observed characteristic patterns arbitrarily adopted as standard. Previous authors have not worked with three dimensional fields, and have expressed two dimensional fields by characteristic patterns of two coordinates of the form $G(\theta, \lambda)$. The separation of variables according to equation 2.1.1 allows a large reduction in the volume of data needed for statistically stable results.

The mean phase velocities were computed in the same way as in the earlier report; the vector correlation method of Ellison (1954) was applied only to satellite cloud data.

2.2 STREAM FUNCTIONS OF THE NORTHERN HEMISPHERE

The stream functions used were operational products of the National Meteorlogical Center at 850, 500 and 200 mb at 0000Z and 1200Z for March 1967. This period was chosen because the best global satellite observations are near the equinoxes. A much longer sequence of data is desirable for future studies with more refined methods.

The points chosen for vertical characteristic patterns lay along a line of longitude, either 100°E - 80°W or 10°E - 170°W.

No check was made for negative absolute vorticities, which are a sign of non-elliptic regions in the operational balance equation, and can occur even in areas of dense data (Bradley, Hayden, and Wiin-Nielsen, 1966). The internal consistency of the results indicates that the effects of negative absolute vorticities are rather small.

2.3 SATELLITE CLOUD DATA

Processing of the brightness and cloud cover to a 5 degree latitude - longitude grid was performed by the National Environmental Satellite Center. The following account is given only for convenient use. Details are given by Bristor, Callicott and Bradford (1966).

The ESSA satellites rotate in nearly sun-synchronous orbits, observing the whole sunlit portion of the earth once per day at approximately the same local time each day and at each longitude. The camera shutter opens only when the optical axis is pointing downwards. Four erase cycles are given to remove about 95% of the previous image from the camera memory. Data is read out on command by certain stations.

The observed brightness is corrected for the camera response as a function of position in the picture, for camera degradation with time, and for the local solar zenith angle. The data is interpolated to a polar stereographic map projection with 64 x 64 points per National Meteorological Center grid square of 381 km side at 60°N. The number of occurrences of each of 5 classes of brightness in an 8 x 8 subset is tabulated, with 64 such histograms per NMC grid square.

A program prepared by Mr. R. Taylor then interpolates the areal average brightness and cloud cover to a 5 degree latitude-longitude grid. In determining the cloud cover, brightnesses in the upper three classes of the histogram are treated as overcast, and the lower two classes as clear. This is believed to give a slight low bias to the cloud cover.

Although some room for improvement remains (for instance in a distinction of cloud origin and small-scale texture), the results given in this report show that the existing data may be used to deduce unexplained atmospheric phenomena. The work reported here is based on operational methods placed in service February 1, 1967. Seasonal cycles and any bias remain for future study.

An attempt was made to apply a correction for camera degradation with time but not with space, as suggested by Mr. J. Winston and Mr. R. Taylor. No change in the deductions of this report was necessitated by these corrections, which caused numerical changes one order of magnitude smaller than the conservative estimated confidence limits of 10 to 20% of the variance. The effects of twighlight observations appear even more important than those of camera degradation, and the apparent non-resolution of at least one physical mechanism (see Chapter 4) seems more important than any correction.

3. RESULTS FROM GEOPOTENTIAL AND STREAM FUNCTION DATA

3.1 RECAPITULATION

It may be recalled briefly that Bradley and Wiin-Nielsen (1967) found the free transient modes of the geopotential of the northern hemisphere to be expressible by the product of zonal harmonics, three pressure modes identical with those reported by Holmström (1963), and four meridional modes with, respectively, 1 to 4 extrema of significant amplitude between 20°N and the pole (Equation 3.5.2 of this report). Removal of the vertical mean suggested that the resultant pressure modes depended slightly on the zonal and meridional wavenumbers, reflecting the variation of tropopause height with latitude. No zonal characteristic patterns could be found. In this report, the vertical modes are denoted by H (for Holmström; 0 for Obukhov (1960) would be confusing), and the meridional modes by L.

When the horizontal expansion was made in surface harmonics (zonal harmonics times associated Legendre polynomials), the mean east-west phase velocity of the weakly divergent first vertical mode H_1 was a Rossby-Haurwitz velocity with an effective meridional wavenumber between 2 and 4. The mean phase velocity of the strongly divergent second vertical mode H_2 varied from the angular velocity of solid rotation of the atmosphere for zonal wavenumbers 1 and 2, to nearly the same value as the first vertical mode H_1 in zonal wavenumber 6.

The first vertical mode H_1 of the free waves resembles the time-mean vertical profile of the zonal mean wind in middle latitudes: the most important vertical effect is thus a change in the strength of the jet, or of wave amplitude.

Although for the free modes of all non-zero zonal wavenumbers the most important meridional variation (L_1) is a change of intensity in middle latitudes, for the zonal mean wind the most important meridional variation (L_2) is a north-south shift of the jet axis. One may take as a working hypothesis the idea that the L_1 mode is related to the index cycle of the westerlies, which is not necessarily uncorrelated to the L_2 mode of the zonal mean geopotential.

The relative importance of the different vertical and meridional modes did not depend on the wavenumber or mode number in any other direction; the scales of the free waves in three directions are independent.

3.2 GYROSCOPIC AND GYROSCOPIC-GRAVITATIONAL MODES

These previous results may be compared with the theory of Dikii (1965), which the author had not then seen. Dikii's theory is linearized about a basic state at rest relative to the earth. It is based on the Laplace tidal equation[1] for a rotating compressible fluid, for which the Rossby-Haurwitz formula is an approximation in a barotropic atmosphere at rest relative to the earth. Dikii's vertical mode equation 3.1 is

$$\partial^2 Y/\partial z^2 + \left[-\tfrac{1}{4} + \frac{\sigma^2 H}{\gamma g}\left(1 - \frac{\gamma H}{h}\right) + \frac{H\beta}{\gamma g h}\right] Y = 0 \qquad 3.2.1$$

where Y is the amplitude, H the height of the homogeneous atmosphere, h an effective depth which depends on the two horizontal wavenumbers, $\gamma = c_p/c_v$ or the ratio of the specific heats of dry air, σ the frequency of oscillation, g is the acceleration due to gravity, and

---

[1] An introductory treatment is given by Eckart (1960).

the stability coefficient

$$\beta = (\gamma - 1)\, g + dc^2/dz \qquad 3.2.2$$

where c is the speed of sound.

As

$$h \approx \gamma H$$

it is seen that the vertical mode structure is predicted to vary slightly with the horizontal wavenumbers. Although no quantitative calculations have been published, Dikii's predictions agree qualitatively with the observations.

Dikii interpreted the first vertical mode H_1 as representing approximately a non-divergent gyroscopic (root 5, or Rossby-Haurwitz) wave, and the higher vertical modes (root 6) as gyroscopic waves modified towards internal gravity waves with longer periods than the Rossby waves. This also agrees with the observations of Bradley and Wiin-Nielsen (1967).

Dikii derived from the Laplace tidal equation an equation for the east-west phase speed of the gyroscopic mode.

$$2\Omega M/\omega = (N+M)\,(N+M+1) + \frac{4A^2\Omega^2}{gh}\,[1/2 + 0\,(1/N) + 0\,(1/M)] \qquad 3.2.4$$

where Ω is the angular velocity of the earth, ω the phase speed in degrees of phase per unit time, M the zonal wavenumber, N the meridional wavenumber, A the radius of the earth, and the other symbols are as before.

If only the first term on the right hand side is retained, equation 3.2.4 reduces to the Rossby-Haurwitz formula. A quantitative comparison is given as Table 3.2.1 (after Golitsin

and Dikii (1966)) with an angular velocity of solid rotation 15.5 degrees longitude per day.

Although the Laplace tidal equation predicts that the movement of the planetary waves will be slower than given by the Rossby-Haurwitz approximation, the effective meridional wavenumber of Bradley and Wiin-Nielsen (1967) cannot be assigned with sufficient precision for a quantitative comparison.

Dikii (1965) gives an equation similar to 3.2.4 for the higher vertical modes, but no numbers have been published.

TABLE 3.2.1

Rotational Speeds of Gyroscopic Modes from Laplace Tidal Equation, Degrees Phase/Day. After Golitsin and Dikii (1966). S is twice the square of (linear velocity of equator/speed of sound).

Legendre Polynomial	P_1^1	P_2^1	P_3^1	P_2^2	P_3^2
Rossby-Haurwitz Period, Days	1	3	6	3	6
R-H Speed	-344.5	-104.5	- 44.5	-104.5	- 44.5
Baroclinic Period, Days S = 7.9	1.17	4.87	8.1	3.22	7.36
Baroclinic Speed S = 7.9	-292.2	- 58.4	- 28.9	-96.0	- 33.4

The Laplace tidal equation for a compressible atmosphere at rest relative to the earth has no roots corresponding to the observed standing and forced parts of the planetary waves.

3.3 MERIDIONAL MODE STRUCTURE

Dikii (1965) gives an equation for the meridional mode structure, but no calculations, and remarks that the solutions may have osculating zeros. The observed characteristic patterns also have

extended regions close to osculating zeros (which is why one must describe them by extrema of significant amplitude) so that one cannot unequivocally equate the sequences of theoretical and observed modes; Longuet-Higgins (1964, 1965, 1967) predicted that the wave packets of the free modes would be confined between two latitudes (which he did not calculate, but which are observed to be about 70°), and gave a qualitative prediction of the existence of forced modes.

3.4 EXPANSION IN CHARACTERISTIC PATTERNS

The standard characteristic H and L patterns of Bradley and Wiin-Nielsen (1967) were used to expand data on the zonal harmonics of the free modes. The phase speeds shown in Table 3.4.1 show that the behavior of the vertical modes of surface harmonics described by Bradley and Wiin-Nielsen (1967) does indeed correspond to the dominant meridional mode. The surface harmonics separate their phase angles only occasionally when a sub-dominant meridional mode becomes temporarily excited. In this case surface harmonics of different meridional wavenumber usually move in the relative direction implied by Table 3.4.1; i.e. for vertical mode 1 the surface harmonic of higher meridional wavenumber moves east relative to the surface harmonic of lower meridional wavenumber, whereas the opposite is true for vertical mode 2. The required relation between the meridional wavenumber and meridional mode number is given by the expansion of the observed modes in surface harmonics, given by Bradley and Wiin-Nielsen (1967).

For vertical mode H_1, meridional mode L_2 moves faster eastward or slower westward than meridional mode L_1, corresponding to a higher effective meridional wavenumber. No way has been found,

however, of defining the concept of effective wavenumber with sufficient precision for any quantitative statement.

For the strongly divergent vertical mode H_2, meridional mode L_2 moves less rapidly eastward than meridional mode L_1, i.e., more nearly resembles its counterpart in the first vertical mode.

TABLE 3.4.1

Observed Mean Phase Speeds of Vertical and Meridional Modes, Degrees Long./Day, from graphs of phase angle against time.

ZONAL WAVE-NUMBER	1		2		3		4		5		6	
VERTICAL MODE	H_1	H_2	H_1	H_2	H_1	H_2	H_1	H_2	H_1	H_2	H_1	H_2
MERIDIONAL L_1	-32.4	14.0	-16.8	16.1	-3.6	13.3	4.0	10.1	9.5	11.1	11.4	9.6
MODE L_2	-13.0	13.3	- 8.8	11.7	7.4	11.6	9.8	9.6	10.9	10.4	11.8	11.1
UNRESOLVED	-32.5	16.0	-16.5	15.0	-3.0	12.0	4.5	11.3	8.8	11.0	7.6	8.4

3.5 EIGENFUNCTIONS OF NON-SELF-ADJOINT OPERATORS

Marchuk (1965, 1967) has developed a theory of frictionless, adiabatic, non-orographic flow using non-self-adjoint linear operators. In this theory, the spectrum of eigen values $\{\lambda_i\}$ and eigenfunctions $\{\psi_i\}$ of a non-self-adjoint operator A does not obey a simple orthogonality relation, but it is possible to define a conjugate operator A* with spectrum $\{\lambda_i^*\}$ and $\{\psi_i^*\}$ such that a biorthogonal relation holds:

$$\psi_i \, \psi_j^* = \delta_{ij} \qquad 3.5.1$$

where δ_{ij} is the Kronecker delta, unity if $i = j$, and zero otherwise.

Data may thus be expressed in terms of the complete but non-orthogonal set of functions $\{\psi_i\}$. The computed $\{\psi_i\}$ are similar to but necessarily not identical with the observed orthogonal characteristic patterns (Marchuk, private communication). The eigenfunctions shown by Gavrilin (1965) do not closely resemble the observed characteristic patterns; Marchuk's result is thus evidence that linearization about a basic state may but does not necessarily cause a substantial departure of the computed from the observed spectrum of characteristic patterns.

The results of Bradley and Wiin-Nielsen (1967), and those reported here, show that the observed modes $\{\phi_o\}$ of the free waves (approximately frictionless, adiabatic and non-orographic) may be expressed as

$$\phi_i(\theta,\lambda,p) = \sum_{j,k,m} H_j(p) L_k(\theta) \exp(im\lambda) \qquad 3.5.2$$

whereas the observed modes of the slowly-moving forced waves cannot be expressed in any form such as 3.5.2. The volume of computation connected with the separation of a three dimensional linear operator into three components by Marchuk (1965, 1967) may be reduced by this observation for the free modes of the planetary waves.

It is observed that the characteristic patterns are much more stable than the corresponding eigenvalues (fractional variance explained). The significance of this result in terms of Marchuk's theory is unknown.

3.6 CHARACTERISTIC PATTERNS OF THE STREAM FUNCTION

The results reported here refer only to the vertical structure at 850, 500 and 200 mb of the NMC operational stream function, twice a day for March 1967, along lines of NMC grid points from

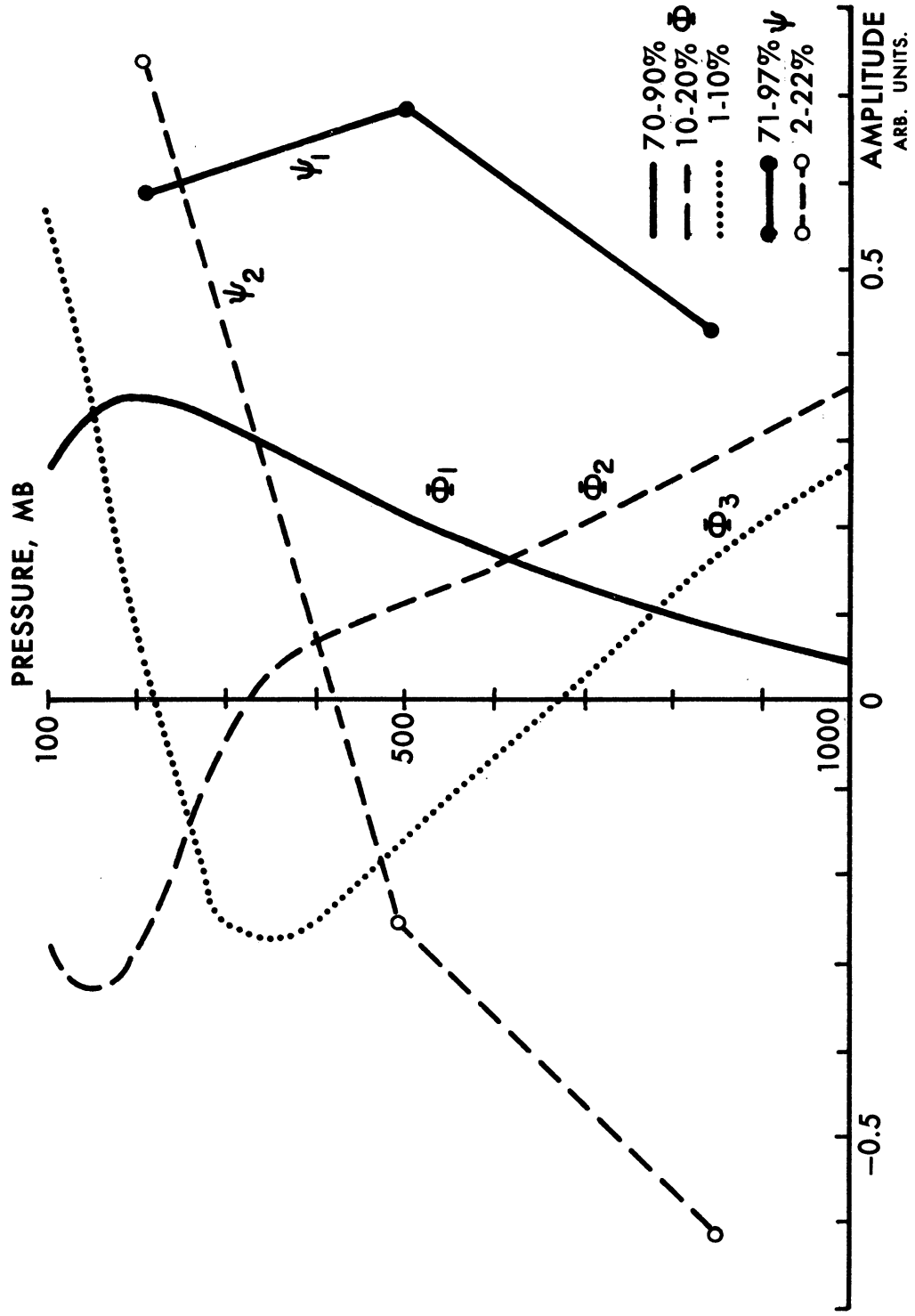

Figure 3.6.1. Characteristic patterns of the geopotential and stream function.

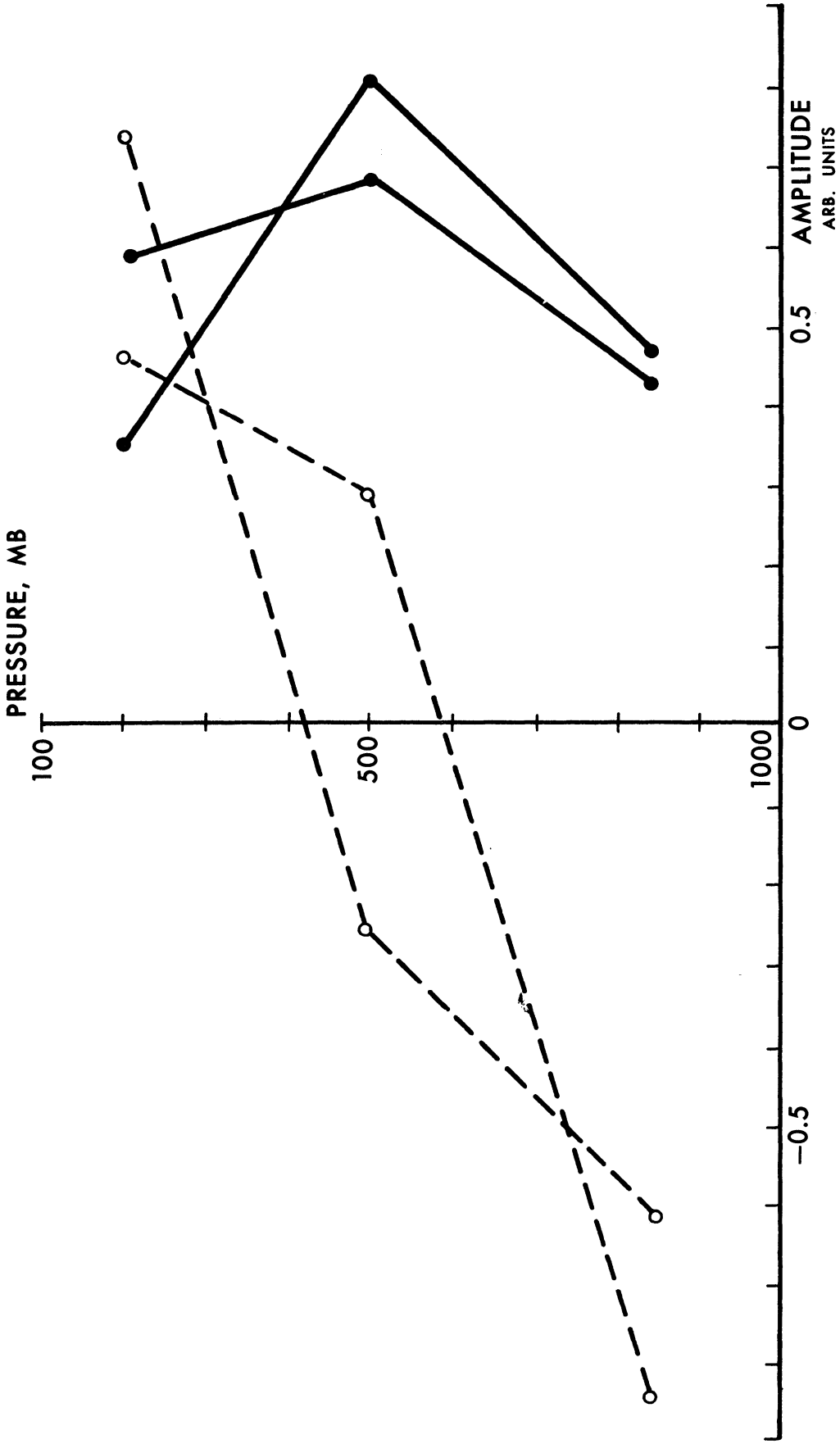

Figure 3.6.2. Characteristic patterns of the stream function at several latitudes.

170°W to 10°E and from 80°W to 100°E, without time filtering. Table 3.6.1 shows values from 170°W to 10°E; the values and meridional variations along 80°W are similar, but the results along 100°E are thought fallacious due to tape handling problems.

As predicted by Bradley (1967), the vertical mode H_2 which is second for the geopotential (10-20% of the variance) is much weaker in the stream function; the author believes that this occurs because this mode is strongly divergent, changing sign in the middle troposphere. The first and second vertical modes of the stream function at three levels on the average explain 87.22 and 9.94% of the variance, respectively.

The first vertical mode is of one sign at all levels, with an extremum at 500 mb (Table 3.6.1); the second vertical mode changes sign in the middle troposphere, and it is almost implied that the third mode has two changes of sign. No deductions should be made from the structure or importance (2.84%) of the third mode. In contrast to the geopotential the first vertical mode of the stream function has its extremum well below 200 mb, and is much larger at 850 mb. The vertical modes of the stream function have no evident relation to the vertical modes of the geopotential with the vertical mean removed, reported by Bradley and Wiin-Nielsen (1967).

The significance of the observed variations with latitude is unknown; it will be necessary to investigate the influence of regions which are non-elliptic for the balance equation, which can cause large negative absolute vorticities in the operational stream function even in regions of dense data (Bradley, Hayden and Wiin-Nielsen, 1966). The variance of the stream function

at 500 mb ranges from 1.2 to 3.5 times the corresponding value at 200 mb; it is unclear to the author whether this reflects a fact of nature.

It is of some interest to remove the vertical mean, because comparable results for the geopotential are given by Bradley and Wiin-Nielsen (1967). In the case of the geopotential, the vertical mean corresponds to a non-divergent part of the geostrophic wind; removal of the vertical mean also accentuated variations corresponding to a change in tropopause height with latitude.

Removal of the vertical mean of the stream function results in the detection of only two vertical modes, which are functions of latitude as shown in Table 3.6.2. The dominant and subdominant modes in low latitudes transform continuously, until at the north pole their structures and importances are exchanged. So far as the author knows, similar behavior has not been reported previously.

TABLE 3.6.1

Structure and Importance of Vertical Modes of the National Meteorological Center Operational Stream Function at NMC Grid Points, 170°W - 10°E, March 1967.

	170°W				10°E			
		Mode				Mode		
Lat.	% Var.	850	500	200	% Var.	850	500	200
19.6	71.14	.149	.607	.780	97.35	.260	.768	.586
	22.24	-.771	-.423	.477	1.82	-.375	-.479	.794
24.7	74.93	.421	.687	.593	96.55	.249	.777	.579
	20.81	-.613	-.266	.744	2.54	-.747	-.227	.625
30.0	89.98	.468	.752	.465	77.51	.101	.978	.182
	6.45	-.689	-.019	.725	3.43	-.873	-.000	.488
35.7	91.81	.458	.775	.435	96.24	.338	.798	.499
	5.96	-.885	.348	.311	2.85	-.894	.106	.436
41.7	89.79	.369	.803	.445	94.76	.348	.807	.478
	8.08	-.908	.271	.319	4.31	-.887	.119	.446
47.9	91.93	.356	.821	.445	91.33	.388	.808	.443
	6.81	-.844	.078	.531	7.62	-.878	.178	.445
54.5	93.05	.456	.811	.365	91.79	.385	.804	.453
	6.40	-.753	.134	.644	6.73	-.857	.129	.500
61.2	94.54	.510	.786	.350	89.55	.411	.764	.498
	4.41	-.707	.152	.690	8.71	-.834	.094	.544
68.2	90.59	.400	.819	.412	79.65	.526	.707	.473
	6.51	-.614	-.094	.784	17.73	-.750	.123	.650
75.4	78.88	.295	.860	.416	75.15	.755	.613	.233
	18.66	-.691	-.109	.714	21.95	-.578	.454	.678
82.7	88.92	.477	.828	.295	88.13	.553	.741	.381
	9.40	-.729	.185	.659	10.35	-.818	.395	.419
90.0	95.63	.465	.811	.355				
	3.00	-.847	.291	.444				

TABLE 3.6.2

Structure and Importance of the Vertical Modes of the National Meteorological Center Operational, Stream Function with the Vertical Mean Removed, 80°W, March 1967.

Lat.	% Var.	MODE 850	500	200
12.6	70.75	.810	-.496	-.314
	29.25	-.105	-.649	.754
32.8	89.38	.816	-.392	-.424
	10.62	.018	-.716	.698
51.2	74.14	.700	-.714	.015
	25.86	-.421	-.396	.816
64.7	68.22	.416	-.816	.401
	31.78	-.704	-.010	.710
79.0	96.76	-.410	-.407	.817
	3.24	.707	-.708	.002
90.0	96.78	-.352	-.444	.824
	3.20	.732	-.680	-.053

4. OBSERVATIONAL RESULTS FROM SATELLITE PHOTOGRAPHS[1]

4.1 VECTOR REGRESSIÓN IN ZONAL AND SURFACE HARMONICS

The method of vector regression described by Ellison (1954) was used to regress one day's changes of the zonal cosine (A) and sine (B) components on the next for zonal and surface harmonics of the brightness and cloud cover, filtered and unfiltered, as described by Deland and Lin (1967). The mean angular velocity may be estimated from the skew-symmetric part of the regression tensor (Deland and Lin, 1967). The estimate is statistically unbiased to the extent that it is immune to random errors. The regressions were performed in zonal harmonics at selected latitudes and in surface harmonics, from February 1 to August 31, 1967. No significant difference was found between cloud cover and brightness.

Table 4.1.1 shows that the mean phase velocity of zonal harmonics depends on latitude, with substantial asymmetry between the hemispheres. The zonal mean wind as a function of latitude, and the mean angular velocity of solid rotation of the entire atmosphere (about 15 deg. longitude/day) have not yet been calculated for the relevant period. The change in the observed speeds with latitude appears to reflect the stronger zonal mean winds of the southern hemisphere which are obvious from any of the films composed of time sequences of satellite photographs; the longest waves move west at 40°N and 25°N, but east at 40°S and 25°S. Erratic apparent speeds occur where the elements of the regression tensor are absolutely small (comparable to the noise level), and can also arise from an insufficient separation of physical mechanisms.

---

[1] Methods are described in Chapter 1 and data in Chapter 2.

TABLE 4.1.1

Regression Tensors, Skew-Symmetric Part, and Mean Angular Velocity in Degrees of Phase per Day. The Angular Velocity may be converted to Deg. Long/Day by Division by the Zonal Wavenumber. The Regression Tensors are for Brightness Deviations from 11 Day Running Means.

Lat.	Z.W.N.	a_{11}	a_{21}	a_{12}	a_{22}	Skew-Symmetric Part		°Ph./Day Dev.	°Ph./Day Raw Data
55°N	1	-.308	-.040	.077	-.298	-.303	-.058	10.9	10.9
	2	-.250	-.154	.101	-.267	-.259	-.127	26.2	24.7
	3	-.272	-.135	.136	-.318	-.295	-.136	24.7	22.3
	4	-.309	-.257	.306	-.306	-.307	-.215	42.5	41.4
	5	-.304	-.203	.319	-.281	-.292	-.261	41.7	45.5
	6	-.299	-.486	.350	-.309	-.304	-.418	54.0	53.0
40°N	1	-.298	.168	-.483	-.141	-.220	.087	-22.0	-18.4
	2	-.225	-.027	.124	-.092	-.158	-.076	25.6	25.5
	3	-.188	-.244	.197	-.261	-.225	-.221	44.4	39.9
	4	-.124	-.217	.200	-.076	-.100	-.209	64.4	59.7
	5	-.131	-.324	.357	.328	-.229	-.340	56.0	52.9
	6	-.162	-.247	.334	-.230	-.196	-.291	56.0	55.3
25°N	1	-.411	.186	-.130	-.288	-.350	.158	-24.3	-22.5
	2	-.201	.061	-.069	-.274	-.238	.065	-15.4	-13.1
	3	-.180	-.040	.070	-.250	-.215	.055	14.3	15.1
	4	-.262	-.163	.036	-.121	-.191	-.100	27.5	39.8
	5	-.081	-.160	-.029	.040	-.060	-.066	47.5	60.5
	6	-.115	-.086	.186	-.062	-.089	-.136	56.9	58.5
10°N	1	-.262	.091	.034	-.327	-.295	.028	-5.5	-11.3
	2	-.364	.018	-.117	-.115	-.239	.068	-15.8	-17.1
	3	-.298	.018	-.027	-.162	-.230	.023	-5.7	-16.2
	4	-.004	-.006	.005	-.339	-.172	-.028	9.3	-4.0
	5	-.199	.107	-.072	-.096	-.147	.089	-31.3	-27.0
	6	-.065	.084	.032	-.197	-.131	.026	11.1	-13.2
10°S	1	-.273	-.111	.058	-.368	-.320	-.085	14.8	13.2
	2	-.388	.011	-.002	-.307	-.347	.006	-1.0	-1.3
	3	-.201	-.102	.049	-.250	-.225	-.075	18.5	21.3
	4	-.208	.026	.029	-.288	-.248	-.002	0.4	7.6
	5	-.076	.180	-.031	-.143	-.140	.024	-12.5	-20.2
	6	-.248	-.067	-.069	.203	-.226	.000	-0.3	-2.9
25°S	1	-.071	-.135	.000	-.287	-.184	-.066	19.9	15.8
	2	-.229	-.001	-.041	-.079	-.154	-.025	9.2	13.3
	3	-.364	-.001	.189	-.082	-.223	-.099	23.9	23.1
	4	-.111	.038	.021	-.132	-.121	.001	-4.1	-8.1
	5	.049	-.223	.134	-.129	-.040	-.179	77.3	68.4
	6	-.258	.014	.075	-.141	-.199	-.031	8.7	10.0
40°S	1	-.289	-.041	.067	-.254	-.271	-.054	11.3	10.4
	2	-.160	-.160	.205	-.037	-.098	-.183	61.7	57.3
	3	-.257	-.184	.142	-.230	-.244	-.163	33.8	31.8

(TABLE 4.1.1 CONT.)

Lat.	Z.W.N.	a_{11}	a_{21}	a_{12}	a_{22}	Skew-Symmetric Part		°Ph./Day Dev.	°Ph./Day Raw Data
40°S	4	-.238	-.189	.227	.397	-.318	.208	33.2	34.1
	5	-.218	-.274	.321	-.142	-.180	-.297	58.8	63.1
	6	-.217	-.523	.409	-.262	.239	-.466	62.8	62.3
55°S	1	-.328	-.228	.322	-.048	-.188	-.275	55.6	53.0
	2	-.065	-.461	.217	-.327	-.196	-.339	60.0	69.1
	3	-.322	-.375	.138	-.294	-.308	-.257	39.8	46.3
	4	-.215	-.389	.364	.324	-.270	-.377	54.6	53.4
	5	-.473	-.163	.354	-.391	-.432	-.258	30.9	31.4
	6	-.344	-.272	.204	-.536	-.440	-.238	28.4	25.7

A method which helped clarify irregularities in the apparent motion of geopotential waves was the use of surface harmonics instead of zonal harmonics (Eliasen and Machenauer, 1965; Deland, 1965). Table 4.1.2 shows the results of this section expressed in surface harmonics; the variation of apparent phase velocity with meridional and zonal wavenumber is not as irregular as its variation with latitude and zonal wavenumber, which suggests that surface harmonics are nearer to the underlying physical mechanisms.

The table 4.1.2 in surface harmonics shows that the time filters used make little difference to the results, which suggests that the slow moving waves cause fast transient cloudiness only by the passage of the fast waves (cyclone families) through them and that the mean phase velocities of the surface harmonics of cloud cover and brightness behave much like the surface harmonics of the geopotential and stream function reported by Eliasen and Machenauer (1965), Deland (1965), and Deland and Lin (1967), Bradley and Wiin-Nielsen (1967), and this report. The waves of largest horizontal scale move west, and the shortest waves tend to the limiting Rossby-Haurwitz velocity of about 15 degrees longitude per day relative to the earth (stationary relative to the solid rotation of the atmosphere). The cloud cover and brightness have phase velocities resembling those of the 2nd meridional mode L_2 of the first vertical mode H_1 of the geopotential as given in Table 3.4.1 of this report, which is evidence for a common mechanism. The motion of large scale clouds must not be interpreted as a wind velocity.

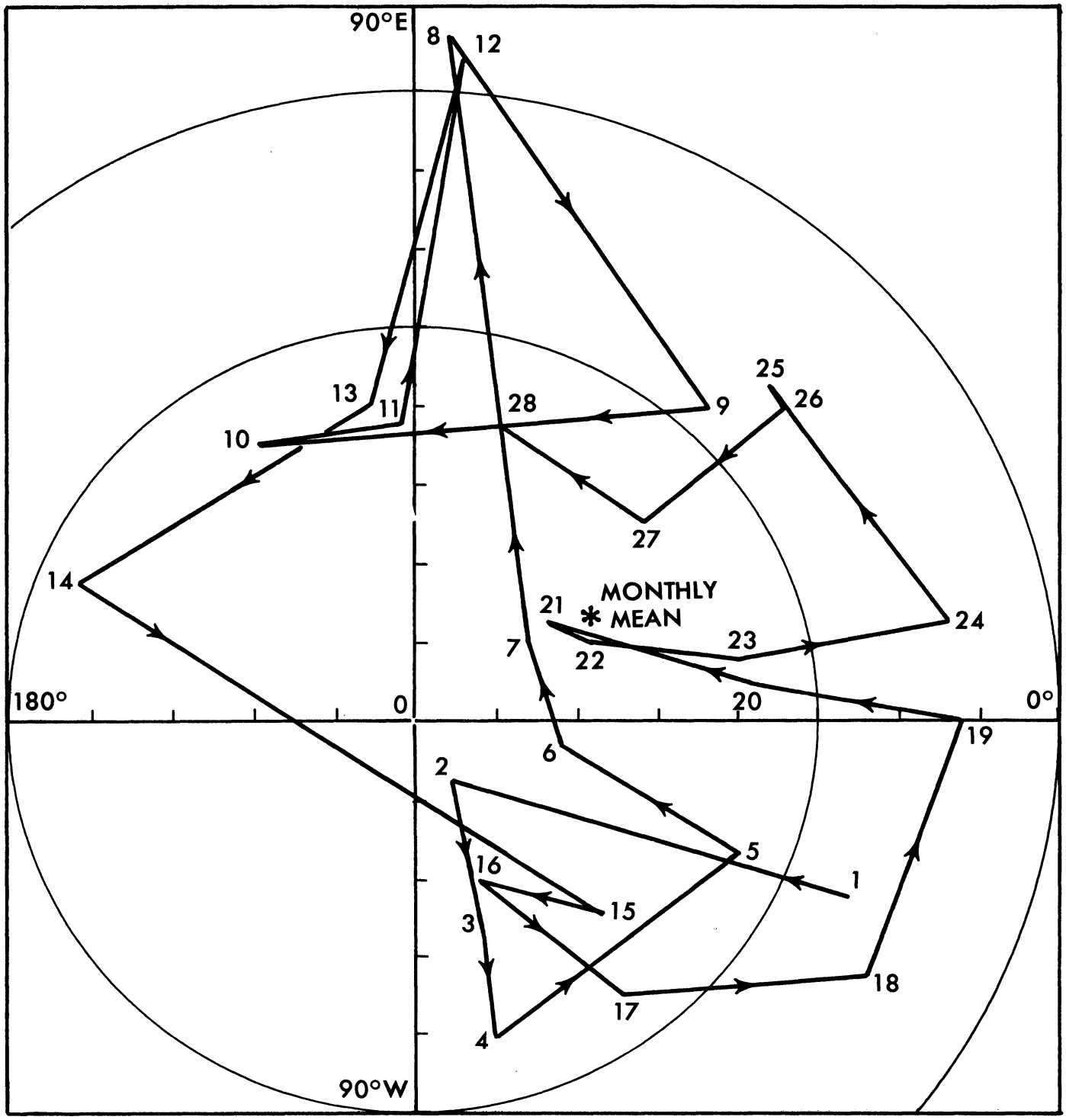

Figure 4.1.1. Harmonic dial of cloud brightness, wave vector (5,4), February 1967.

TABLE 4.1.2

As Table 4.1.1, but in Surface harmonics.

M.W.N.	Z.W.N.	Deg. Phase/Day Deviations	Deg. Phase/Day Raw Data
0	1	-12.0	-11.3
	2	-6.8	-6.0
	3	8.8	11.9
	4	37.9	34.4
	5	2.3	4.2
	6	43.2	30.0
1	1	7.2	3.1
	2	-10.0	-9.0
	3	-2.6	-3.5
	4	59.1	56.0
	5	38.9	53.8
	6	33.3	32.5
2	1	-3.9	-6.5
	2	13.8	29.1
	3	14.4	26.2
	4	63.7	63.5
	5	44.7	40.6
	6	60.1	61.1
3	1	15.4	15.0
	2	9.6	21.7
	3	71.3	71.3
	4	46.1	44.6
	5	58.2	52.5
	6	55.3	52.2
4	1	10.5	13.4
	2	5.2	6.7
	3	50.8	48.5
	4	59.8	69.2
	5	63.3	61.2
	6	61.5	59.1
5	1	3.3	4.1
	2	52.4	51.2
	3	27.3	27.4
	4	38.4	41.4
	5	61.1	64.4
	6	62.3	63.9

Much vacillation is evident from the low values of the elements in the regression tensor; for uniform rotation at constant amplitude, the sum of squares of the two skew-symmetric elements would be 1.0. Monthly values of the mean angular velocity, and the examination of machine plotted harmonic dials lead to the same conclusion.

It should be remembered that, if the interhemispheric coupling were weak, then calculating the mean phase velocities of surface harmonics by quadrature of the entire sphere would be little more than a formalistic exercise. In such a case, calculations should be made for each hemisphere separately, with artificial symmetry about the equator. Section 4.2 presents evidence that this is not the case.

4.2 ZONAL HARMONIC CHARACTERISTIC PATTERNS OF LATITUDE

No significant differences were found between cloud cover and brightness at the present 5 to 10% level of subjective confidence in interpretation of variance expalined.

On the basis of preliminary results, the globe was examined as a whole and in latitude belts from 55°N to 55°S, 55°N to 20°N, 20°N to 20°S, and 20°S to 55°S. This avoided a large part of the meteorologically trivial effects due to the motion of the polar night boundary with time; the most convincing results for the whole globe are obtained near the equinoxes, probably because of poor camera response in twilight areas. Another objective was to allow modes confined to the tropics to show themselves instead of being swamped by consideration of the whole sphere. These new techniques met with substantial success, as judged by the increase in the largest eigenvalue and the case-to-case stability of the modes identified. The results obtained, however, have obviously

not completely separated all the physical effects, and it is not reasonable to define any standard modes for an expansion of data in orthogonal functions.

In order to determine how much of the results were likely to be due to deficiencies of the camera, telemetry, mal-location of data, imperfect solar zenith angle corrections, and other systematic or contingent data errors, all observed modes were compared with the mean values for the corresponding period. In no case does any mode resemble the mean values sufficiently to prevent interpretation at the confidence level of 5 to 10% in variance explained. The author does not know of any statistical method of evaluating such effects, nor of any objective method of establishing a level of confidence. Unless otherwise stated, the author believes the deductions of this report to be influenced insignificantly by deficiencies of the data collection and reduction system.

Most of the observed meridional modes of zonal harmoics have several extrema of opposite signs; such modes could be generated by a simple model system of a zonal harmonic of which the phase angle varied continuously over a multiple of 2π between the poles. A simple east-west rotation of such a hypothetical system would lead to meridional modes resembling those observed. To test this possibility, both the amplitude and the sine-cosine coefficients were examined; the observed modes are not significantly different in the two cases, so that the deductions of this report can contain only small contributions due to a meridional tilt in ridge and trough lines.

Both the raw data and the deviations from an 11 day running mean of both the brightness and the cloud cover exhibit charac-acteristic patterns with one and two significant extrema between

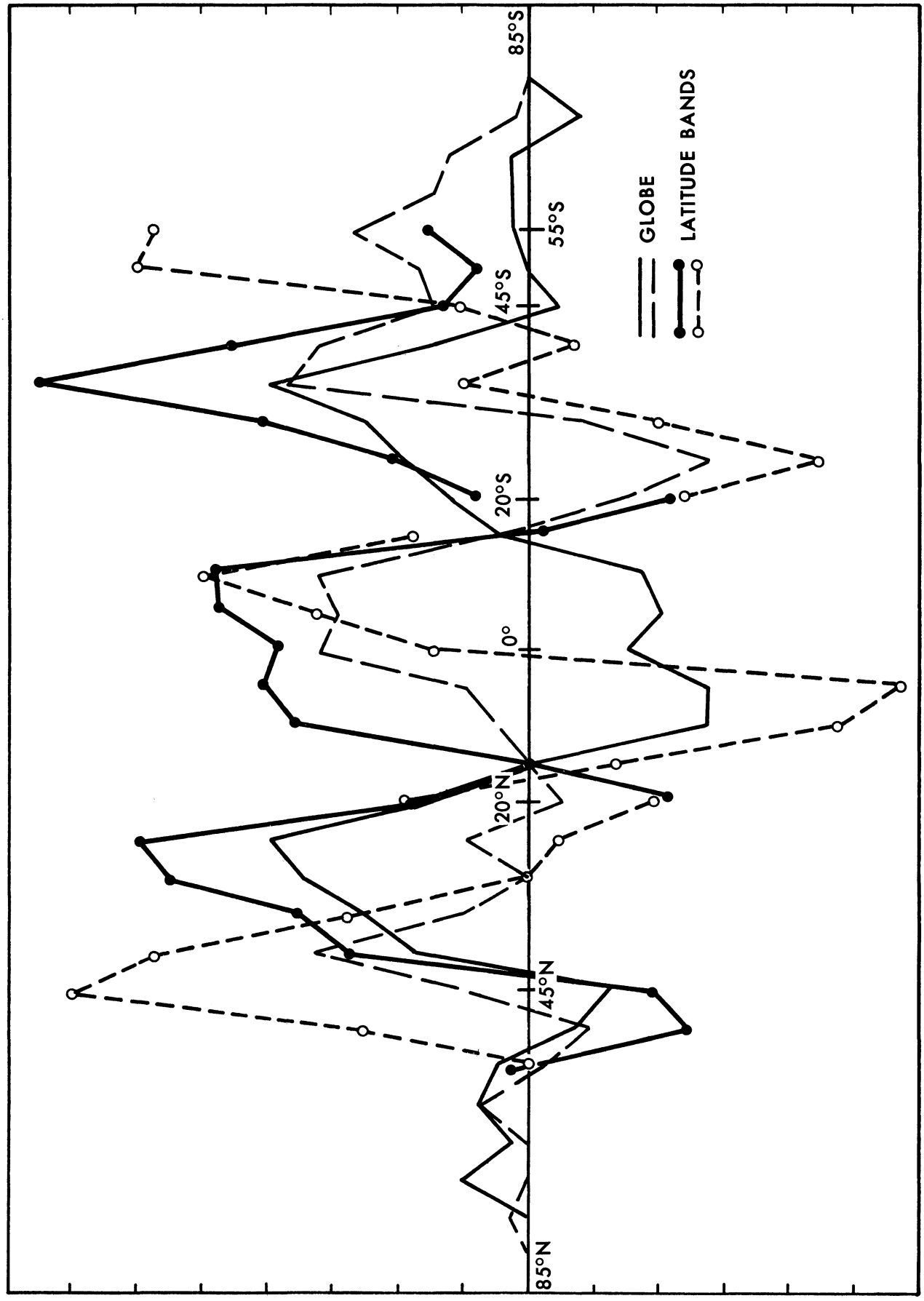

Figure 4.2.1. Meridional characteristic patterns of cloud brightness, March 1967.

latitudes 55 and 20, in both the northern and southern hemispheres considered separately. The extrema coincide approximately with those observed for the geopotential (Bradley and Wiin-Nielsen, 1967). The lack of statistical stability prevents any statement about higher meridional modes at present. In contrast to the results for the geopotential, the zonal mean cloud cover and brightness exhibit a single-extremum mode indistinguishable from the corresponding meridional mode of any other zonal wavenumber. For all zonal wavenumbers (except zero) the two-extremum meridional mode of the cloud cover and brightness is about as important as the one-extremum mode; see Table 4.2.1.

TABLE 4.2.1

Fractional Variance Explained by 1 and 2 - Extremum Meridional Modes. Brightness, Raw Data and Deviations, March 1967.

Data	Merid.	Z.W.N.					
Raw	Mode	0	1	2	3	4	5
Globe	1	.821	.229	.276	.224	.265	.285
	2	.073	.165	.149	.144	.152	.141
N.H.	1	.879	.448	.437	.325	.368	.349
	2	.046	.190	.197	.304	.235	.297
Trop.	1	.766	.311	.438	.404	.411	.467
	2	.078	.267	.230	.195	.262	.185
S.H.	1	.882	.318	.380	.326	.425	.460
	2	.047	.259	.261	.270	.218	.179
Dev.							
Globe	1	.501	.173	.200	.179	.220	.236
	2	.111	.153	.152	.165	.142	.181
N.H.	1	.414	.308	.394	.378	.448	.473
	2	.260	.230	.221	.219	.170	.197
Trop.	1	.458	.310	.333	.350	.313	.298
	2	.176	.222	.212	.194	.169	.199
S.H.	1	.733	.323	.344	.306	.299	.389
	2	.121	.224	.251	.254	.230	.244

The deviation from the running mean generally have only a quarter to a half of the variance of the raw data (Table 4.2.2), but are more influenced by quasi-random noise.

TABLE 4.2.2

Variance (Arbitrary Units) of Raw Brightness Data, and Deviations from 11 Day Running Means, March 1967.

Data	Z.W.N.						
Raw		0	1	2	3	4	5
	Globe	342.7	107.5	102.5	120.1	99.1	110.2
	N.H.	85.8	37.6	33.5	39.9	27.5	34.6
	Trop.	53.8	35.3	29.5	39.8	32.9	38.9
	S.H.	103.0	33.8	36.2	42.6	39.6	41.1
Dev.							
	Globe	70.0	65.3	70.4	78.6	59.4	72.8
	N.H.	13.7	19.0	21.3	27.5	23.0	26.3
	Trop.	16.6	22.3	20.6	24.9	15.6	16.2
	S.H.	32.5	22.8	25.5	27.1	20.0	28.4

The approach to couplings between the hemispheres and to the tropics is rather crude in this study, and is based on the behavior of characteristic patterns. Nevertheless, the author does not know of any published estimates of the order of magnitude of such coupling. Ignoring the fortuitous interchanges of dominance order between modes of comparable importance, the dominant meridional

characteristic patterns of either hemisphere and of the tropics are the same as those of the globe as a whole. The main effects are therefore coupled over the entire world. The author considers it probable that the instantaneous phase velocities of the planetary wave include significant effects from the whole sphere; such a conclusion does not necessarily hold for mean phase velocities given elsewhere in this report. The coupling does not necessarily imply large exchanges of matter, energy and angular momentum: it may only be necessary to couple two systems with about the same free period.

The uncoupled modes may be estimated as the change of the largest eigenvalues for the whole sphere and the several latitude belts (Table 4.2.1). Uncoupled modes explain on the average 10 to 20% of the variance. This estimate is crude, and not based on careful statistics, but it gives a previously unknown order of magnitude.

Symmetric and anti-symmetric modes appear to be of comparable importance, with the symmetric mode more important in the longest waves. Large fluctuations in the corresponding eigenvalues are observed, however. Because characteristic patterns are uncorrelated as well as orthogonal, the symmetric and anti-symmetric modes cannot be explained by assuming that waves in the two hemispheres move with approximately equal but uncoupled speeds.

Modes essentially confined to the tropics explain about 10% of the variance in the tropical belt; such modes are observed by consideration of the sphere as a whole. Although one must be careful about equating the observed modes to those predicted by Lindzen (1967) and Matsuno (1966) because their structure is not

well described and their phase velocities are still unknown, the author considers it a probable working hypothesis that weak tropical modes exist.

The results presented in this section show a definite advantage in the representation of east-west structure in zonal harmonics, rather than leaving it unresolved. The poor statistical stability of the results is thought, by analogy with cases studied previously, probably to represent a failure to resolve one or more distinct physical mechanisms. The poor statistical stability cannot be attributed mainly to noise; although the failure to resolve the type and height of clouds, and to recognize snow, may well be part of the story, the author is inclined to think that inability to resolve the strongly divergent second vertical (H_2) mode of the first latitudinal (L_1) mode may be the main problem. The observed motions of the large scale cloudiness resemble those of the (H_1, L_2) mode of the geopotential in magnitude and in their variation with wave vector, but the vertical motions connected with the (H_2, L_1) mode are not necessarily much less important.

4.3 POWER SPECTRA AND FILTERING

Power spectrum analyses of the brightness raw data were made for zonal wavenumbers 0 to 5 at 10° intervals of latitude from 60°N to 60°S from February 1 to May 31, and from June 1 to August 29, 1967, with lags of 0 to 30 days by 2 day steps.

Nearly all the spectra have three distinct peaks corresponding to periods of 15 to 30 days, 3 to 6 days, and 2 to 2.5 days. The picture is thus similar to that assumed by Bradley and Wiin-Nielsen (1967), and the separation of physical processes by a 5.5 day, 10.5 day or 11 day running mean time filter is confirmed. The 3

Table 4.3.1

Power Spectra of Brightness Raw Data, Feb. 1 to May 31, 1967. Mean Removed. N Days of Lag Represent a Period of 60/N Days.

		Days of Lag (Maximum used 30).													
Z.W.N.	Lat.	2	4	6	8	10	12	14	16	18	20	22	24	26	28
0	50N	1.189	1.819	.448	.297	.167	.226	.181	.095	.087	.092	.157	.105	.128	.138
	20N	2.258	.937	.565	.236	.351	.398	.150	.045	.069	.090	.096	.060	.064	.084
	0	2.004	.669	.405	.356	.267	.224	.183	.141	.096	.093	.153	.111	.148	.184
	20S	2.004	.700	.461	.312	.249	.205	.151	.109	.085	.100	.102	.060	.138	.150
	50S	18.406	2.364	.764	.552	.407	.294	.186	.161	.149	.171	.253	.131	.317	.342
1	50N	1.303	.407	.170	.149	.109	.110	.147	.143	.122	.119	.210	.263	.155	.165
	20N	.400	.603	.680	.594	.228	.159	.231	.346	.323	.115	.069	.065	.074	.098
	0	.489	.403	.261	.250	.392	.336	.122	.142	.161	.102	.082	.071	.123	.153
	20S	.194	.289	.306	.255	.323	.310	.192	.115	.062	.087	.088	.067	.068	.073
	50S	.453	.139	.167	.176	.208	.215	.163	.220	.184	.150	.142	.126	.153	.165
3	50N	.659	.362	.277	.188	.139	.191	.235	.260	.222	.084	.095	.085	.131	.281
	20N	1.917	.933	.384	.410	.426	.371	.243	.133	.156	.235	.168	.071	.074	.103
	0	.217	.269	.463	.482	.421	.410	.322	.238	.247	.146	.126	.154	.107	.098
	20S	.456	.314	.357	.342	.246	.124	.115	.110	.105	.086	.063	.103	.153	.146
	50S	.411	.376	.420	.285	.155	.202	.218	.183	.177	.158	.159	.167	.232	.307
5	50N	.324	.290	.234	.296	.380	.233	.263	.414	.333	.164	.154	.178	.154	.121
	20N	.804	.471	.147	.296	.339	.401	.479	.230	.054	.024	.050	.042	.053	.067
	0	.556	.547	.313	.210	.192	.186	.215	.256	.282	.232	.171	.115	.071	.122
	20S	.464	.751	.586	.187	.167	.256	.249	.200	.148	.099	.044	.044	.051	.059
	50S	.225	.338	.336	.199	.201	.248	.337	.441	.244	.133	.229	.299	.348	.215

to 6 day peak is thought to be a quasi-Rossby-Haurwitz velocity, but the 2 day peak is strongly suspected to be a modulation of the data caused by the fact that the satellite orbital period is not a simple sub-multiple of 24 hours.

Power spectra have not yet been evaluated for any geopotentials, stream functions, cloud cover, nor for any orthogonal functions other than zonal harmonics. Power spectrum analysis of the brightness deviations from an 11 day running mean confirms the satisfactory separation of the 15 to 30 day and 3 to 6 day peaks.

Power spectrum analysis of surface harmonics over 212 days does not alter the above deductions, but separates the seasonal modes from the other forced modes.

4.4 GROUPING OF ZONAL WAVENUMBERS

Although Bradley and Wiin-Nielsen (1967) were unable to identify any zonal characteristic patterns significantly different from zonal harmonics, this result could not be assumed to apply to cloud parameters. In particular, the existence of cyclone families on the east sides of the planetary wave troughs suggests that there might be some relation between different wave-numbers. Two arbitrary groupings of zonal wavenumbers were adopted.

No such relation could be identified for either brightness or cloud cover, irrespective of whether the data was time filtered. Two groupings of zonal wavenumbers were tried, each over all 35 latitudes and over the two mid-latitude belts and tropics separately. In the first scheme, zonal wavenumbers 0-3, 4-7, 8-11, 12-15 were grouped, and in the second, wavenumbers (0,4,8,12), (1,5,9,13), (2,6,10,14), (3,7,11,15). Four wavenumbers at 35 latitudes require a 140 by 140 covariance matrix; the program occupied 172K of core

TABLE 4.4.1

Illustrative Eigenvectors for the Meridional Variation of Grouped Zonal Wavenumbers. Brightness, interpolated for missing days but not time filtered.

Lat.	(1) Mode 2 8.42%	(2) Mode 2 6.33%	(3) Mode 2 9.31%	(4) Mode 2 7.61%	(5) Mode 2 4.56%	(6) Mode 2 13.91%
55°N	-.79623	-.12075	-.71668	.07622	-.04028	.01096
	.04048	.06038	.08231	-.01127		
	.02692	.00791	-.12562	.04613		
	.19955	.03475	-.06939	.04631		
50°N	-.16155	.01100	-.18282	-.05186	.28707	-.47420
	.05819	.01627	.16886	-.11296		
	-.01984	.03570	.19681	.14012		
	-.08459	-.02268	-.06463	.14644		
45°N	.12096	.17362	.07785	-.21181	-.28127	-.59670
	-.09335	.03156	.01187	-.20827		
	-.00010	.08227	.18914	.12739		
	-.01289	-.00861	.00503	.03860		
40°N	.09129	.37557	.04951	-.29141	-.09627	.17564
	-.08615	.01636	.00049	-.07453		
	-.02556	.04193	.02054	.11825		
	.07350	.08155	.02317	-.06670		
35°N	.18139	.44472	.12568	-.32409	-.13079	.40942
	.03948	-.05185	-.01716	-.12177		
	-.01911	.12985	.09105	.21562		
	-.00667	.10537	.00195	-.06836		
30°N	.27875	.23295	.20026	-.23217	.28643	.43441
	.09213	.02311	.00744	-.15227		
	.10471	.01074	-.03824	.23186		
	-.04909	.00686	.04464	.03404		
25°N	.08267	-.32272	.04004	.18936	.54201	.16903
	.00317	.02944	.01304	.08998		
	.13660	-.04134	-.02825	.28369		
	-.05035	.00124	.16933	-.00460		
20°N	.21679	-.61501	.17238	.45644	.64545	-.05661
	-.01392	.05180	.00233	.23739		
	.19034	-.12693	-.03034	.11586		
	.03621	-.05284	.42196	-.11310		

(1) Feb. 1 to May 1, 1967. Wavenumbers 0, 4, 8, 12
(2) May 2 to July 30, 1967. Wavenumbers 0, 4, 8, 12
(3) Feb. 1 to May 1, 1967. Wavenumbers 0, 1, 2, 3
(4) May 2 to July 30, 1967. Wavenumbers 0, 1, 2, 3
(5) March 3 to April 1, 1967. Wavenumber 0
(6) June 1 to June 30, 1967. Wavenumber 0

TABLE 4.4.2

Comparison of Variance Explained by Separate and Grouped Zonal Wavenumbers. Percentage and Total Variance (Arbitrary Units) are Stated.
Cloud cover, interpolated for missing days, but not time filtered, 55°N to 20°N.

		Groups	Single Zonal Harmonics		
		Feb. 1 to May 1, 1967	Feb. 1 to March 2, 1967	March 3 to April 1, 1967	April 2 to May 1, 1967
1 Group:	0	50.71% (823.85)	49.55% (75.56)	82.95% (90.54)	47.34% (32.52)
	1		30.88% (56.41)	40.53% (47.08)	37.96% (36.26)
	2		57.92% (73.32)	53.80% (53.73)	34.81% (32.86)
	3		37.35% (55.76)	34.83% (57.08)	31.48% (34.83)
2 Group:	0	56.82% (706.18)	49.55% (75.56)	82.95% (90.54)	47.34% (32.52)
	4		37.19% (59.23)	36.68% (37.28)	45.02% (37.97)
	8		—	—	—
	12		—	—	—

storage and ran about 11 minutes of central processor time on the Control Data 6600. In view of the large size, long running time, and evidence obtained from the 256 schemes (2 methods of grouping, 4 groups, 4 latitude blocks, 2 time periods, cloud cover and brightness, raw data or deviations from a running mean) tried, this was considered enough.

Table 4.4.1 shows some illustrative eigenvectors obtained, although no statistics were collected, it is clear from the tendency for the absolutely largest elements at each latitude to correspond to the same zonal wavenumber that the results are not substantially different from zonal harmonics.

Table 4.4.2 lists for identical data the fractional variance explained by the dominant linear combination of zonal wavenumbers, and the fractional variance explained by the dominant mode of the dominant wavenumber in the linear combination. Single wavenumbers give sharper results than groups of wavenumbers, because of the blurring which arrises when statistics are performed over physically separate effects.

4.5 CHARACTERISTIC PATTERNS OF LATITUDE AND LONGITUDE

Because the author believes that the existence of cyclone families should cause correlations between the planetary waves, even though these correlations are so weak and unstable that their statistical detection amid other physical effects has not been achieved, characteristic patterns of longitude were evaluated at selected latitudes. The cases comprised (1) brightness and cloud cover, (2) running 11 day mean and deviation, (3) 5 latitudes, 50°N by 25° to 50°S, and (4) the whole circle, and superpositions in halves, thirds, quarters and sixths.

The variance explained by the first mode rarely exceeds 20%, which is an indicator of extreme statistical instability. Some improvement is obtained by superposing subdivisions of the latitude circle, but the results remain open to the gravest doubts. Comparison of the observed modes along different latitude circles, and along one latitude circle at different times, confirms these doubts. The results do not, however, resemble the mean values for the corresponding time periods.

Meridional characteristic patterns were evaluated along a given longitude. The whole longitude, and latitudinal blocks 55°N to 20°N, 20°N to 20°S, and 20°S to 55°S were chosen. The results again did not resemble the mean values, and the 1 and 2 extremum modes reported in section 4.3 dominated the picture for both cloud cover and brightness, and for both raw data and deviations. The percentage variance explained by the dominant mode was usually about half that obtained from the meridional C.P.'s of zonal harmonics. It is therefore concluded that zonal harmonics give a simpler representation of physical processes than functions expressed at grid points.

4.6 STRUCTURE AND CORRELATION FUNCTIONS

Zonal and meridional structure and correlation functions of the brightness raw data, and of the deviation from an 11 day running mean, were computed for several base latitudes and longitudes by 30 day periods. The results are neither homogeneous nor isotropic in space; Tables 4.6.1 through 4.6.4 list two specimens of each function for the same time period. The specimens are not normalized in any way.

TABLE 4.6.1

Meridional Structure Functions of Cloud Brightness, March 1967. Based on longitude 0°, latitudes 40°N and the Equator. Not normalized.

Lat.	70°N	60	50	40	30	20	10	0	10	20	30	40	50	60	70°S	
40°N	390	369	305	0	100	226	313	378	328	214	193	427	655	645	127	(1)
0°	296	348	510	378	227	266	174	0	195	281	256	450	574	731	558	(1)
40°N	202	223	133	0	38	79	91	260	91	95	53	70	170	224	125	(2)
0°	368	468	309	260	196	244	167	0	217	232	225	266	288	402	166	(2)

(1) Raw Data
(2) Deviations

TABLE 4.6.2

Meridional Correlation Functions, same data as Table 4.6.1

Lat.	70°N	60	50	40	30	20	10	0	10	20	30	40	50	60	70°S	
40°N	7	131	344	312	209	198	53	107	26	157	131	315	330	384	406	(1)
0°	38	125	226	107	130	162	107	280	76	107	83	312	354	325	174	(1)
40°N	-7	-7	22	47	8	9	-2	-20	-6	-7	6	-3	-17	-14	22	(2)
0°	-27	-67	-3	-20	-8	-11	23	173	-7	-14	-13	1	7	-55	25	(2)

TABLE 4.6.3

Zonal Structure Functions, same data as Table 4.6.1

Long.	10	20	30	40	50	60	80	100	120	140	160	180	160	140	120	100	80	60	50	40	30	20	10°W
40°N	167	432	365	874	667	341	349	187	317	524	459	583	363	265	549	390	487	616	364	375	139	159	188(1)
0°	221	281	301	230	278	214	246	178	300	218	335	258	259	252	250	235	274	373	428	280	226	200	208(1)
40°N	93	149	221	131	178	129	170	101	176	294	274	247	98	121	199	248	262	193	111	221	71	107	105(2)
0°	291	293	320	187	195	173	191	234	193	235	302	164	176	176	183	177	192	355	230	231	184	149	234(2)

TABLE 4.6.4

Zonal Correlation Functions, same data as Table 4.6.1

Long.	0	10	20	30	40	50	60	80	100	120	140	160	180	160	140	120	100	80	60	50	40	30	20	10°W
40°N	312	184	121	274	461	306	267	267	249	143	298	313	225	420	200	197	198	330	298	285	272	214	180	255(1)
0°	278	162	151	145	46	1	49	46	114	180	211	134	14	12	16	3	33	151	182	224	147	99	121	121(1)
40°N	47	19	8	-23	-2	-8	1	-24	4	0	-11	-14	-9	9	-1	-21	-15	1	23	26	4	17	9	15(2)
0°	173	-7	-11	-49	-44	-7	11	-1	-4	21	8	-12	7	-1	-1	-1	-1	3	-37	-3	15	4	35	34

If the existence of characteristic patterns had not been known, then these results would have compelled their invention. The results can amount to no more than a single characteristic pattern, but they do show the existence of substantial correlations over 30° of latitude and 180° of longitude. There is no evidence that the structure functions of the brightness tend to a limit at sufficiently large distances from any reference point; their behavior is oscillatory even at very large distances.

The structure and correlation functions of cloud brightness therefore differ from those of the geopotential reported by Gandin (1963) in a way which makes them unusable but reinforces the idea of characteristic patterns.

5. CONCLUSIONS

5.1 INTER-HEMISPHERIC COUPLING AND CLOUD SYSTEM KINEMATICS

The characteristic patterns indicate that the two hemispheres and the tropics are strongly coupled, with uncoupled modes accounting for only 10 to 20% of the variance. Statistically uncorrelated symmetric and anti-symmetric modes are of approximately equal importance. Large exchanges of matter and energy are not necessarily implied, and there is no suggestion that single hemisphere forecast models cannot be highly successful.

Problems with the polar night boundary and with inadequate data in areas of low sun severely restrict the periods when good results for the whole sphere can be obtained.

The observed meridional modes of cloud cover and brightness resemble those previously reported for the geopotential, but are not sufficiently statistically stable to be used in the expansion of data. Cloud data has not been expanded in the observed meridional modes of the geopotential, but expansions in surface harmonics indicate that the main component of the large scale cloudiness moves with the quasi-Rossby-Haurwitz velocity of the first vertical mode H_1 of the second meridional mode L_2 of the geopotential. This fact has obvious implications for the interpretation of cloud motions as wind velocities, and for the type of information which present techniques of machine analysis would contribute to global meteorlogical analysis. Further work is needed to see whether the quasi-stationary forced modes and any other free modes (including the dominant meridional mode L_1 of the geopotential) can be analyzed automatically.

Analyses in zonal harmonics show a definite advantage over attempts to identify zonal characteristic patterns.

5.2 TROPICAL MODES

It is probable that weak tropical modes were identified, but their description remains too statistically unstable for any quantitative comparison of their structure and motion with the available theories.

5.3 DYNAMICS OF PLANETARY WAVES

Although no numbers have been published for the modes predicted by the available theories based on the Laplace tidal equation and on the spectra of non-self-adjoint linear operators, the observed motions of the free planetary waves are qualitatively consistent with the theory of mixed internal-gravitational and gyroscopic waves. Nothing in any linearized perturbation theory corresponds to the observed standing and quasi-stationary forced modes. Problems will arise for models formulated in theoretical or observed modes because the observed meridional characteristic patterns of the free (adiabatic, frictionless, non-orographic) modes differ from those of the forced modes, especially near the poles.

Power spectra of zonal harmonics of the cloud brightness support the existence of two peaks at 15 to 30 and 3 to 6 days. A third peak at 2 days is thought to be a defect in the data.

A vertical mode which changes sign in the middle troposphere is much less important for the stream function than for the geopotential, which supports the idea that a large part of the atmospheric divergence is connected with the second vertical mode of the geopotential. Nevertheless, the first vertical mode

of the geopotential appears sufficiently dominant to control the motions of the planetary scale cloudiness.

6. SUGGESTIONS FOR FUTURE WORK

6.1 DIAGNOSTIC EXTENSIONS TO SATELLITE DATA

The use of characteristic patterns for dynamic studies based on satellite observations requires a knowledge of their relation to the vertical velocities in the atmosphere and to the divergence of the horizontal windfield. Relations should therefore be sought between cloud patterns and the vertical H and horizontal modes L of the geopotential and of the stream function. At the same time one may test the working hypothesis that the L_1 mode of the waves is related to the index cycle and to the L_2 mode of the zonal mean geopotential. The second (strongly divergent) vertical mode H_2 of the geopotential is much weaker in the stream function. On the other hand, the divergence and hence the vertical velocity are expected to be closely related to the large scale cloudiness.

When these relations have been understood from the study of simultaneous satellite and conventional data in the northern hemisphere, it will be necessary to expand data in standard functions in order to diagnose the dynamics and interactions of the tropics and southern hemisphere.

Such a knowledge may one day allow observations of clouds and thermal radiation to be used in the diagnosis of energetic effects and in the generation of initial state analyses for numerical forecast models.

6.2 THEORY

The most promising theoretical work for the derivation of the eigenfunctions of atmospheric variables is the method of non-self-adjoint linear operators described by Marchuk (1965, 1967).

It will be necessary to understand the relation between the bi-orthogonal spectra of such operators and the observable orthogonal characteristic patterns.

It will also be useful to have prognostic models using characteristic patterns, in order to elucidate their maintenance and the significance of non-linear interactions, mountains, friction and diabatic effects which are represented only with substantial approximations in existing theories. The author makes the working hypothesis that the characteristic patterns of the free gyroscopic and gyroscopic-gravitational planetary waves are almost independent of the detailed laws of friction and diabatic heating, which serve only as slowly acting sources and sinks of energy. Conversely, characteristic patterns are expected to give no information about the laws of friction, and to give new information about diabatic effects only through a knowledge of the physical laws of scattering, absorption and emission of radiation.

APPENDIX A

BEHAVIOR OF CHARACTERISTIC PATTERNS

1. DEFINITIONS

The material in this section is not original; see Mateer (1965), Anderson (1958). The meteorologist familiar with characteristic patterns will find original material in the other sections of Appendix A.

Consider some system X_j defined at M points in space ($j = 1, 2, \ldots M$) as a function of time, and suppose that it can be described by N functions V_{ij}, $i = 1, 2, \ldots, N$, $j = 1, 2, \ldots M$ which do not vary with time t (the simplest case is M = 1 and $V_{ij} = 1$).

Then by definition

$$X_j = \sum_{i=1}^{N} b_i(t)\, V_{ij} \qquad , j = 1,2,\ldots M \qquad \text{A.1}$$

where the coefficients b_i are functions only of time.

Let a bar ($\overline{\quad}$) denote a time average, and form the square, symmetric covariance matrix Y with non-negative main diagonal

$$Y_{ij} = \overline{X_i X_j} = \left(\sum_{K=1}^{N} b_K V_{Ki} \sum_{L=1}^{N} b_L V_{Lj}\right) \qquad \text{A.2}$$

$$= \sum_{K=1}^{N} \sum_{L=1}^{N} \overline{b_K b_L}\, V_{Ki} V_{Lj}$$

Now, any symmetric matrix of order M may be expressed in the form used for deflation (Fadeev and Fadeeva, 1960, Sect. 59) in terms of its eigenvalues λ_K and eigenvectors U_K, $K = 1, 2, \ldots M$. The M eigenvalues λ_K are scalars, and each of the M eigenvectors has M elements.

$$Y_{ij} = \sum_{K=1}^{M} \lambda_K U_{Ki} U_{Kj} \qquad , i, j = 1,2,\ldots,M \qquad \text{A.3}$$

The eigenvalues of a symmetric matrix with a non-negative main diagonal are all real and non-negative, obeying

$$Y\, U_K = \lambda_K\, U_K \qquad \text{A.4}$$

Numerous methods of determining eigenvalues and eigenvectors are described in every textbook on numerical analysis (Fox, 1964; Fadeev and Fadeeva, 1960).

Equations A.2 and A.3 therefore differ in the presence of cross-product terms

$$\overline{b_K\, b_L\, V_{Ki}\, V_{Lj}} \quad , K \neq L \qquad \text{A.5}$$

in A.2. Also, the vectors V are not necessarily orthogonal, whereas the eigenvectors U obey an orthonormality relation

$$V_i\, V_j = \delta_{ij} \quad \begin{matrix} = 0 & \text{if } i \neq j \\ = 1 & \text{if } i = j \end{matrix} \qquad \text{A.6}$$

Further, if one makes an expansion (which is possible under all circumstances of interest in meteorology)

$$X_j = \sum_{i=1}^{n} g_i\,(t)\, U_{ij} \qquad \text{A.7}$$

then

$$\overline{g_i^2} = \lambda_i \qquad \text{A.8}$$

$$\overline{g_i\, g_j} = 0 \quad \text{if} \quad i \neq j \qquad \text{A.9}$$

and thus the eigenvalues of the covariance matrix Y are proportional to the variance explained by the corresponding eigenvectors, and the eigenvectors are statistically uncorrelated over the dependent data sample. The eigenvectors are variously called modes, empirical

orthogonal functions, characteristic patterns, principal components, principal factors or natural functions. The equations A.3 and A.7 are uniquely defined by the covariance matrix Y; there are always infinitely many possible expansions of the form A.1, but the properties of orthogonality and non-correlation often make the characteristic pattern method more convenient. The spectrum of a non-self-adjoint linear operator (Marchuk, 1967) is a special case of equation A.1 in which the f_i are uncorrelated but the V_{ij} are not orthogonal. Expansions in analytic orthogonal functions (e.g. sines and cosines, or surface harmonics) are orthogonal but not uncorrelated.

Nothing requires that $\overline{f_i}$ or $\overline{g_i}$ be zero or non-zero: in the study of the dynamics of planetary waves, however, the author has always removed the sample mean in order to remove the standing and forced modes, so that

$$\overline{f_i} = \overline{g_i} = 0 \qquad , i = 1, 2, \ldots, M \qquad \text{A.10}$$

Consider the correlation coefficients implied by equation A.7

$$\overline{X_i X_j} = \left(\sum_{K=1}^{N} g_K U_{Ki} \sum_{L=1}^{N} g_L U_{Lj}\right) = \sum_{K=1}^{N} \lambda_K U_{Ki} U_{Kj} \qquad \text{A.11}$$

from equations A.8 and A.9

The correlation coefficient

$$R_{ij} = \overline{X_i X_j} / \left(\overline{X_i X_i} \ \overline{X_j X_j}\right)^{1/2}$$
$$= \sum_{K=1}^{N} \lambda_K U_{Ki} U_{Kj} / \left(\sum_{K=1}^{N} \lambda_K U_{Ki}^2 \sum_{K=1}^{N} \lambda_K U_{Kj}^2\right)^{\frac{1}{2}} \qquad \text{A.12}$$

is not necessarily non-zero, and may be computed from a knowledge of the eigenvalues and eigenvectors of the covariance matrix. It is left as an exercise for the reader to show that the geopotentials at 120 mb and 920 mb are virtually uncorrelated, using the modes and variances given in Section 3.6.

Data at M points is normally sufficient to give a solution of the set of equations A.7 for the coefficients g_{ij}; the value of the variable X at any other point may then be determined.

It is left as an excercise to the reader to show that a simplification to two of the observed vertical modes of the geopotential with variances in the ratio of 6:1, allows the geopotential at 120 mb to be computed from the geopotentials at 500 mb and 920 mb with approximately equal and opposite weights, even though the predictand is uncorrelated with one of the predictors.

A knowledge of characteristic patterns enables one to select predictors adequate to determine the coefficients in any particular specimen of data; these predictors thus give the value of any point in the region of interest. Prediction equations based on characteristic patterns are stable against changes in the relative importance of modes (as happened to the geopotential in the early part of 1963; see Bradley and Wiin-Nielsen, 1967), but not against changes in the modes. The possible applications of characteristic patterns to objective analysis have not been explored; all work known to the author is in terms of regressions, correlation functions, or structure functions (Gandin, 1963).

Eigenvectors are arbitrary to a multiplicative constant,; the conventional normalization is given by equation A.6. The eigenvalues of a covariance matrix are most conveniently normalized so that

their sum is unity:

$$\sum_{K=1}^{M} \lambda_K = 1.0 \qquad \text{A.13}$$

This may be achieved by dividing the covariance matrix by the sum of the elements on its main diagonal, called the spur or trace.

$$Sp\,(Y) = \sum_{K=1}^{M} Y_{KK} \qquad \text{A.14}$$

On this definition,

$$Y_{ij} = \overline{X_i X_j} \Big/ \sum_{K=1}^{M} \overline{X_K{}^2} \qquad \text{A.15}$$

2. DIAGNOSTIC USES

Characteristic patterns are an optimum set for the description of a physical system, in a least squares sense. They may also be advantageous for meteorological forecast models because it is known that nature does not accumulate energy in any other modes. Any model which does not reflect the variance observed to be explained by each mode is in error. Diagnostic calculations of the energetics of forecast models and of nature may conveniently be made in standard characteristic patterns. The adequacy of their definition may be tested by their statistical stability from one data sample to another.

3. ORTHOGONALITY PROPERTIES

Characteristic patterns are orthogonal over the parameters which define the covariance matrix (pressure levels, latitudes, longitudes, etc.), because they are the eigenvectors of the covariance matrix. It follows that the effect of adding or deleting parameters (changing the order of the covariance matrix) depends

on the position of the parameters relative to the zeros and the extrema of the characteristic patterns. For instance, consider a system with two significant, well defined modes such that one mode is near zero where the other mode is large, and vice versa; such a system is the geopotential at 500 and 1000 mb (Bradley and Wiin-Nielsen, 1967). The addition of a third level substantially alters the observed functions, yet if enough levels are considered it is found that the addition of many levels may have little influence, as is illustrated by the fact that Bradley and Wiin-Nielsen (1967) found the same three modes from eight pressure levels as Holmström (1963) found from 37 levels.

Because the higher modes of a system explain the least variance, are less statistically stable than the dominant modes, and in many cases represent phenomena of smaller scale, it is usually found that the higher modes are affected by changes in the volume of data and number of parameters considered. The dominant modes are affected by changes in the volume of data and the number of parameters only when the volume of data is not sufficiently large to eliminate fortuitous correlations, when the parameters are not optimally defined, or when the changes introduce a large change in the system variance, e.g. when the polar night boundary is excluded from characteristic patterns of the brightness.

New artifices to alleviate this situation are introduced in this report. Some of the observed phenomena are interpreted as meaning that inter-hemispheric couplings are rather weak, and that a substantial part of the short term fluctuations in cloudiness occur as the fast transient waves pass certain preferred longitudes dictated by the slow moving waves. Further, fortuitous correlations between the fast moving waves of the two hemispheres cannot be avoided if

one considers time periods short enough for the slow moving waves to be regarded as quasi-stationary. Because no practical method has yet been published for referring data to axes based on the slow moving waves, and because long (several years) time series are not available, the situation was clarified by using 30 day time series, running mean filters, and a separation into three blocks of latitudes.

4. MACHINE PROCESSING DIFFICULTIES

Difficulties in machine processing of characteristic pattern results arise from the fact that the sign is arbitrary and unpredictable, and from interchanges of modes of comparable importance. The absolute value of the dot product of normalized functions is the best guide to mode identification. The number of zeros or of extrema is difficult to use automatically, because of fortuitous small fluctuations and because of regions which may be close to zero.

5. STANDARD FUNCTIONS

Once some set of modes has been chosen as standard, they may be used to expand data in the same way as any other set of orthogonal functions. The only difficulty which arises is that modes are uncorrelated over the dependent data sample from which they were derived, but not necessarily over an independent data sample. Consequently, weak subordinate modes cannot necessarily be described when data is expanded in a set of standard characteristic patterns. The third vertical mode described by Bradley and Wiin-Nielsen (1967) illustrates this problem: the fact that the phase angles of the first and third vertical modes were always close together arises solely from the replacement of observed modes by standard modes, and does not reflect any phenomenon of nature.

BIBLIOGRAPHY

Anderson, T. W., 1958: An Introduction to Multivariable Statistical Analysis. John Wiley, 374 pp.

Baer, F., 1964: Integration with the Spectral Vorticity Equation. Journal of the Atmsopheric Sciences, 21, No. 3, 260-276.

Belousov, S.L., 1956: Tablitsi Normirovanikh Prisoedinennikh Polinomov Lezhandra. Akademiya Nauk SSSR. Reprinted as: Normalized Associated Legendre Polynomials; Mathematical Tables Series vol. 18. Pergamon, 1962.

Blackman, R. B. and J. W. Tukey, 1959: The Measurement of Power Spectra. Dover, 190 pp.

Blinova, E.N., 1943: Gidrodinamicheskaya Teoriya Voln Davleniya, Temperaturnikh Voln i Tsentrov Deistviya Atmosferi. Dokladi Akademii Nauk SSSR, 39, no. 7, 284-287. (A Hydrodynamic Theory of Pressure and Temperature Waves and the Centers of Action of the Atmosphere.)

Blinova, E.N., 1964: Long Range Hydrodynamic Weather Forecasting. Israel Program for Scientific Translations, 1965, 123 pp.

Blinova, E.N., 1975: Dinamika Atmosfernikh Dvizhenii Planetarnogo Masshtaba i Gidrodinamicheskoi Dolgosrochnii Prognoz Pogodi. Trudi Mirovogo Meteorologicheskogo Tsentra, vip. 5, 84 pp. (The Dynamics of Atmospheric Planetary Scale Motions and Hydrodynamic Long Period Weather Forecasting.)

Bradley, J. H. S., C. M. Hayden, and A. C. Wiin-Nielsen, 1966: An Attempt to Use Satellite Photography in Numerical Weather Prediction. University of Michigan, Office of Research Administration, Report 07424-1-T.

Bradley, J. H. S, 1967: The Transient Parts of the Atmospheric Planetary Waves. Proceedings of the (Seventh) Stanstead Seminar on the Middle Atmosphere. Arctic Meteorology Research Group, Dept. of Meteorology, McGill University.

Bradley, J. H. S. and A. C. Wiin-Nielsen, 1967: The Transient Part of the Atmospheric Planetary Waves. University of Michigan, Project Report 06372-5-T.

Bristor, C. L., W. M. Callicott and R. E. Bradford, 1966: Operational Processing of Satellite Cloud Pictures by Computer. Monthly Weather Review, 94, No. 8, 515-527.

Burger, A. P., 1958: Scale Considerations of Planetary Motions of the Atmosphere. Tellus, 11, 195-205.

Charney, J. G., 1947: The Dynamics of Long Waves in a Baroclinic Westerly Current. Journal of Meteorology, 4, no. 5

BIBLIOGRAPHY (continued)

Charney, J. G. and A. Eliassen, 1949: A Numerical Method for Predicting the Perturbations in the Middle-Latitude Westerlies. Tellus, 1, no. 2, 38-54.

Deland, R. J., 1965a: Some Observations of the Behavior of Spherical Harmonic Waves. Monthly Weather Review, 93, no. 5, 307-312.

Deland, R. J., 1965b: On the Scale Analysis of Travelling Planetary Waves. Tellus, 17, no. 4, 527-528.

Deland, R. J., and Yeong-jer Lin, 1967: On the Movement and Prediction of Traveling Planetary-Scale Waves. Monthly Weather Review, 95, no. 1, 21-31.

Derome, J. F. and A. Wiin-Nielsen, 1966: On the Baroclinic Stability of Zonal Flow in Simple Model Atmospheres. University of Michigan, Project Report 06372-2-T.

Dikit, L. A., 1961: Natural Oscillations of a Baroclinic Atmosphere Above a Spherical Earth. Izvestya A.N.SSSR, no. 5, 756-765.

Dikit, L. A., 1965: The Terrestrial Atmosphere as an Oscillating System. Izvestiya A.N. SSSR, Ser. Atm. i Okean. Fiz., 1, No. 5, 469-489.

Eckart, C., 1960: Hydrodynamics of Oceans and Atmospheres. Pegamon Press, 290 pp.

Eliasen, E., and B. Machenauer, 1965: A Study of the Fluctuations of the Atmospheric Planetary Patterns Represented by Spherical Harmonics. Tellus, 17, no. 2, 220-238.

Ellison, T. H., 1954: On the Correlation of Vectors. Quarterly Journal of the Royal Meteorological Society, 81(343), 93-96.

Fadeev, D. K. and V. N. Fadeeva, 1960: Computational Methods of Linear Algebra. W. H. Freeman, 1963, 621 pp.

Fox, L., 1964: An Introduction to Numerical Linear Algebra. Oxford University Press, 328 pp.

Gandin, L. S., 1963: Obektivnii Analiz Meteorologicheskikh Polei. Gidrometeoizdat. Translated as: Objective Analysis of Meteorological Fields. Israel Program for Scientific Translations, 1965.

Gavrilin, B. L., 1965: On the Description of the Vertical Structure of Synoptic Processes. Izvestiya Akademii Nauk SSSR, Seriya Atm. i Okean. Fiziki, No. 1, 8-17.

Golitsin, G. S. and L. A. Dikii, 1966: Oscillations of Planetary Atmospheres as a Function of the Rotational Speed of the Planet. Izvestiya A.N SSSR, ser. Atm. i Okean. Fiz., 2, no. 3, 225-235.

Holloway, J. L., 1958: Smoothing and Filtering of Time Series and Space Fields. Advances in Geophysics, Vol. IV, pp. 351-389. Academic Press.

Holmstrom, I., 1963: On a Method for Parametric Representation of the State of the Atmosphere. Tellus, 15, No. 2, 127-149.

Holopainen, E. O., 1966: A Diagnostic Study of the Maintenance of Stationary Disturbances in the Atmosphere. University of Michigan, Office of Research Administration Report 06372-3-T.

Lindzen, R. D., 1967: Planetary Waves on Beta Planes. Monthly Weather Review, 95, no. 7, 441-451.

Longuet-Higgins, M. S., 1965: Planetary Waves on a Rotating Sphere II. Proc. Roy. Soc. A284, 40-68.

Longuet-Higgins, M. S., 1964: Planetary Waves on a Rotating Sphere. Proc. Roy. Soc. A279, 446-473.

Longuet-Higgins, M. S. and A. E. Gil, 1967: Resonant Interactions between Planetary Waves. Proceedings of the Royal Society, Series A, 299 (1456), 120-140.

Marchuk, G. I., 1965: O Chislennom Reshenii Zadach Prognoza Pogodi. In: Dynamics of Large Scale Processes, Proceedings of the International Symposium, Moscow, June 23-30, 1965. Izdatelstvo Nauka, Moscow, pp. 58-66.

Marchuk, G. I., 1967: Chislennie Metodi v Prognoze Pogodi. Gidrometeoizdat, Leningrad, 356 pp. It is understood that french and english translations will be published.

Mashkovich, S. A., 1961: K. Teorii Voln Davleniya v Baroklinoi Atmosfere. Trudi Tsentralnogo Instituta Prognozov, Vipusk 111, 13-28.
(On the Theory of Pressure Waves in a Baroclinic Atmosphere.)

Mashkovich, S. A., 1964a: Obektivnii Analiz Aerologicheskikh Nabliudenii i Trebovanie k Razmeschcheniya Seti Stantsii. Izvestiya Akademii Nauk SSSR, Seriya Geofizicheskaya, No. 2, 285-292.

Mateer, C. L., 1965: On the Information Content of Umkehr Observations. Journal of the Atmospheric Sciences, 22, no. 4, 370-381.

BIBLIOGRAPHY (continued)

Matsuno, T., 1966: Quasi-Geostrophic Motions in the Equatorial Area. Journal of the Meteorological Society of Japan, 44, No. 1, 25-42.

Murakami, T., 1963: Analysis of Various Large Scale Disturbances and the Associated Zonal Mean Motions in the Atmosphere. Geofisica Pura e Applicata, 54, 119-165.

Obukhov, A. M., 1960: O Statisticheski Ortogonalnikh Razlozheniyakh Empiricheskikh Funktsii. Izvestiya Akademii Nauk SSSR, Seriya Geofizicheskaya, No. 3, 432-439. (On Statistically Orthogonal Expansions in Emperical Functions.)

Robert, A., 1966: The Integration of a Low Order Spectral Form of the Primitive Meteorological Equations. J. Met. Soc. Japan, 44, No. 5, 237-245.

Smagorinsky, J., 1953: The Dynamical Influence of Large-Scale Heat Sources and Sinks on the Quasi-Stationary Mean Motions of the Atmosphere. Quarterly Journal of the Royal Meteorological Society, 79, 342-366.

Yaglom, A. M., 1953: Dinamika Krupnomasshtabnikh Protsessov v Barotropnoi Atmosfere. Izvestiya A.N. SSSR, ser. Geofiz., no. 4, 346-369.

Yang, C. H., 1967: Nonlinear Aspects of the Large-Scale Motion in the Atmosphere. Univ. of Mich., Project Report 08759-1-T.